

# The structure of POMGNT2 provides new insights into the mechanism to determine the functional *O*-mannosylation site on $\alpha$ -dystroglycan

Rieko Imae<sup>1</sup> | Naoyuki Kuwabara<sup>2</sup> | Hiroshi Many<sup>1</sup> | Tomohiro Tanaka<sup>3</sup> |  
Masato Tsuyuguchi<sup>2</sup> | Mamoru Mizuno<sup>3</sup> | Tamao Endo<sup>1</sup> | Ryuichi Kato<sup>2</sup> 

<sup>1</sup>Molecular Glycobiology, Research Team for Mechanism of Aging, Tokyo Metropolitan Geriatric Hospital and Institute of Gerontology, Itabashi-ku, Japan

<sup>2</sup>High Energy Accelerator Research Organization (KEK), Institute of Materials Structure Science, Structural Biology Research Center, Tsukuba, Japan

<sup>3</sup>Laboratory of Glyco-organic Chemistry, The Noguchi Institute, Itabashi-ku, Japan

## Correspondence

Ryuichi Kato, KEK, Photon Factory,  
Structural Biology Research Center,  
1-1 Oho, Tsukuba, Ibaraki 305-0801, Japan.  
Email: ryuichi.kato@kek.jp

Tamao Endo, Molecular Glycobiology,  
Research Team for Mechanism of Aging,  
Tokyo Metropolitan Geriatric Hospital and  
Institute of Gerontology, 35-2 Sakae-cho,  
Itabashi-ku, Tokyo 173-0015, Japan.  
Email: endo@tmig.or.jp

## Present address

Naoyuki Kuwabara, PeptiDream Inc,  
Kawasaki, Japan

## Funding information

This work was supported by the Japan Society for the Promotion of Science Grants (JSPS) KAKENHI JP19H05648 (to T.E., and R.K.), JP17H03987 (to H.M.), JP16K07284 (to N.K.); and the Japan Agency for Medical Research and Development (AMED) 20am0101083j0004 (to R.K.), 17gm0810010h0202 (to H.M.), 21ek0109443h0002 (to H.M.).

**Communicated by:** Hitoshi Kurumizaka

## Abstract

Defects in the *O*-mannosyl glycan of  $\alpha$ -dystroglycan ( $\alpha$ -DG) are associated with  $\alpha$ -dystroglycanopathy, a group of congenital muscular dystrophies. While  $\alpha$ -DG has many *O*-mannosylation sites, only the specific positions can be modified with the functional *O*-mannosyl glycan, namely, core M3-type glycan. POMGNT2 is a glycosyltransferase which adds  $\beta$ 1,4-linked GlcNAc to the *O*-mannose (Man) residue to acquire core M3-type glycan. Although it is assumed that POMGNT2 extends the specific *O*-Man residues around particular amino acid sequences, the details are not well understood. Here, we determined a series of crystal structures of POMGNT2 with and without the acceptor *O*-mannosyl peptides and identified the critical interactions between POMGNT2 and the acceptor peptide. POMGNT2 has an N-terminal catalytic domain and a C-terminal fibronectin type III (FnIII) domain and forms a dimer. The acceptor peptide is sandwiched between the two protomers. The catalytic domain of one protomer recognizes the *O*-mannosylation site (TPT motif), and the FnIII domain of the other protomer recognizes the C-terminal region of the peptide. Structure-based mutational studies confirmed that amino acid residues of the catalytic domain interacting with mannose or the TPT motif are essential for POMGNT2 enzymatic activity. In addition, the FnIII domain is also essential for the activity and it interacts with the peptide mainly by hydrophobic interaction. Our study provides the first atomic-resolution insights into specific acceptor recognition by the FnIII domain of POMGNT2. The catalytic mechanism of POMGNT2 is proposed based on the structure.

## KEYWORDS

core M3, fibronectin type III domain, glycosyltransferase, muscular dystrophy,  $\alpha$ -dystroglycanopathy

Rieko Imae and Naoyuki Kuwabara contributed equally

This is an open access article under the terms of the Creative Commons Attribution-NonCommercial-NoDerivs License, which permits use and distribution in any medium, provided the original work is properly cited, the use is non-commercial and no modifications or adaptations are made.

© 2021 The Authors. *Genes to Cells* published by Molecular Biology Society of Japan and John Wiley & Sons Australia, Ltd.

## 1 | INTRODUCTION

The dystrophin-glycoprotein complex (DGC) is a plasma membrane-localized protein complex that connects components of the extracellular matrix (ECM), such as laminin, with the actin cytoskeleton. In muscles, DGC is thought to provide physical stability to the sarcolemma, and deficiency of the DGC components is the cause of muscular dystrophies, a heterogeneous group of genetic disorders that cause progressive muscle weakness.  $\alpha$ -Dystroglycan ( $\alpha$ -DG), a key component of the DGC, is present on the cell surface and binds to the ECM components.  $\alpha$ -DG is modified with *O*-mannosyl glycan, a type of *O*-glycan in which the reducing terminal mannose (Man) is attached to proteins via side chains of Ser or Thr residues.  $\alpha$ -DG is highly glycosylated with *O*-mannosyl glycans on its mucin-like domain (residues 316–485) (Harrison et al., 2012; Nilsson et al., 2010; Stalnaker et al., 2010). The *O*-mannosyl glycans are classified into three core structures based on the linkage of GlcNAc to the *O*-Man residue: core M1 (GlcNAc $\beta$ 1-2Man), core M2 [GlcNAc $\beta$ 1-2(GlcNAc $\beta$ 1-6)Man], and core M3 (GalNAc $\beta$ 1-3GlcNAc $\beta$ 1-4Man) (Chiba et al., 1997; Endo, 2019; Sheikh et al., 2017; Yoshida-Moriguchi et al., 2013; Manya & Endo, 2017; Inamori et al., 2004).  $\alpha$ -DG from skeletal muscle contains many core M1-type glycans, but it is the core M3-type glycan which is essential for binding to the ECM components (Endo, 2019; Manya & Endo, 2017; Sheikh et al., 2017). To date, it has been reported that three specific positions on  $\alpha$ -DG, that is, Thr317, Thr319, and Thr379, can be modified with core M3-type glycan (Hara et al., 2011; Yoshida-Moriguchi et al., 2010; Yagi et al., 2013).

The synthesis of *O*-mannosyl glycan is initiated in the endoplasmic reticulum (ER) by protein *O*-mannosylation via POMT1/POMT2 (Manya et al., 2004). During the core M1 synthesis, the GlcNAc $\beta$ 1-2Man structure is formed by protein *O*-mannose *N*-acetylglucosaminyltransferase 1 (POMGNT1) in the Golgi (Yoshida et al., 2001). Then, various peripheral structures are formed on core M1 (Harrison et al., 2012; Morise et al., 2014; Harrison et al., 2012; Nilsson et al., 2010; Stalnaker et al., 2010). Meanwhile, the core M3 structure is synthesized in the ER by the addition of  $\beta$ 1,4-linked GlcNAc to the initial Man residue by POMGNT2 and the addition of GalNAc to the GlcNAc by B3GALNT2 (Yoshida-Moriguchi et al., 2013). Afterward, a Man residue is phosphorylated at the C6 position by POMK (Yoshida-Moriguchi et al., 2013), and  $\alpha$ -DG is transported to the Golgi, where core M3-type glycan is further modified. In the Golgi, the first ribitol phosphate (RboP) is transferred to the GalNAc by FKTN, and the second RboP is transferred to the first RboP by FKR, to form a tandem RboP structure (Kanagawa et al., 2016). Then, a GlcA $\beta$ 1-4Xyl $\beta$ 1-4 unit is formed by the sequential action of RXYLT1 and B4GAT1 (Manya et al., 2016; Praissman et al., 2014; Willer et al., 2014). Finally, the

(-3GlcA $\beta$ 1-3Xyl $\alpha$ 1-) repeating unit, which is required for the binding to the ECM components (Yoshida-Moriguchi & Campbell, 2015), is synthesized by LARGE (Inamori et al., 2012), forming a functional core M3-type glycan. All genes encoding the enzymes involved in the core M3-type glycan synthesis are associated with  $\alpha$ -dystroglycanopathy, a group of muscular dystrophies with neuronal abnormalities (Endo, 2019; Manya & Endo, 2017; Sheikh et al., 2017).

As described above, three specific *O*-Man positions on  $\alpha$ -DG are modified by POMGNT2 in the ER, and the remaining *O*-Man residues are modified by POMGNT1 in the Golgi. This suggests that POMGNT2 selects the specific *O*-Man residues in advance of POMGNT1 action. Previously, Halmo *et al.* reported that POMGNT1 is promiscuous for *O*-mannosylated peptides, whereas POMGNT2 displays significant primary amino acid selectivity near the site of *O*-mannosylation (the TPT motif). They also proposed that the RXR motif at the N-terminal side of the *O*-Man-modified residue contributed to the acceptor selectivity of POMGNT2 (Halmo et al., 2017). However, elimination of RXR had only moderate effects on the POMGNT2 activity (Halmo et al., 2017). This indicates that the POMGNT2 acceptor selectivity is not explained solely by the presence or absence of the RXR motif. Other critical amino acid sequences or motifs for the recognition by POMGNT2 are unknown. In addition, POMGNT2 is known to contain a unique fibronectin type III (FnIII) domain (Manzini et al., 2012). According to the Cazy database, in vertebrates, POMGNT2 is the only glycosyltransferase that has an FnIII domain, but its function is unclear. In addition, how GlcNAc is transferred from UDP-GlcNAc to the *O*-Man residue of  $\alpha$ -DG by POMGNT2 is unsolved. To better understand how POMGNT2 recognizes the substrates, including the functional role of the FnIII domain, we here performed a structural study of POMGNT2 and elucidated recognition mechanisms of donor and acceptor substrates. We found that an acceptor substrate was sandwiched between the two protomers of POMGNT2 dimer. We then show the importance of both the *O*-mannosylation site (TPT motif) and the hydrophobic residues at the C-terminal side of the *O*-Man-modified residue. These amino acids are recognized by both the catalytic domain and the characteristic FnIII domain of POMGNT2. Finally, we propose the catalytic mechanism of POMGNT2.

## 2 | RESULTS

### 2.1 | Structure of POMGNT2 consisting of catalytic and FnIII domains

A soluble form of bovine POMGNT2 (sPOMGNT2, residues 45–580) was expressed in HEK293S GnT- cells, purified, and crystallized. The phase information of the crystal was

determined experimentally by the iodide-SAD method using an NaI-soaked crystal (Appendix S1: Table S1). POMGNT2 belongs to the GT61 glycosyltransferase family in the Cazy database, and this is the first crystal structure in the GT61 family of proteins. There are two sPOMGNT2 (molecules A and B) and two UDP molecules in the asymmetrical unit (Figure 1a and Appendix S1: Figure S1a). The structures of the two sPOMGNT2 protomers are almost identical (the r.m.s.d. of the C $\alpha$  carbon is 0.317 Å). The two protomers interact with each other via 24,847 Å<sup>2</sup> as determined by ePISA (Krissinel & Henrick, 2007). This tight interaction suggests that POMGNT2 functions as a dimer.

One sPOMGNT2 molecule consists of an N-terminal catalytic domain (residues 53–476) and a C-terminal FnIII domain (residues 477–580) (Figure 1b). The catalytic domain is composed of two Rossmann-like folds (N-lobe and C-lobe), as expected for a GT-B fold that is widely found in glycosyltransferases (Breton et al., 2006). We could build the crystal structure of the N-lobe (residues 53–277) and C-lobe (residues 286–476) in both protomers, but we could not build a loop region connecting them (residues 278–285) due to the poor electron density. FnIII domains have been found in many intracellular and extracellular proteins among diverse species (>7,800 in UniProt lists), and many of them include an extended array of FnIII (Maurer et al., 2015), but sPOMGNT2 has a single FnIII domain. The FnIII domain interacts with the N-lobe of another protomer of sPOMGNT2 and forms a domain-swapped dimer (Figure 1a). In addition, the N-lobes of two protomers interact with each other and contribute a dimer formation. These two interactions lead to the formation of a wide protomer-protomer interface.

## 2.2 | Catalytic active site

The UDP molecule, which is thought to be carried over from cultivated cells, was found in the catalytic domain (Figure 1a,b and Appendix S1: Figure S1). The UDP is located in the groove formed by the N-lobe and C-lobe, just as in the other GT-B glycosyltransferases. In the C-lobe of sPOMGNT2, a unique insertion (residues 395–451) is found, which is conserved among POMGNT2 orthologues but not in other typical GT-B glycosyltransferases (Appendix S1: Figure S2) (Lairson et al., 2008). The groove around the active site of sPOMGNT2 is larger than those of other GT-B glycosyltransferases via an interaction of the insertion region with part of the N-lobe (residues 247–251).

Three charged amino acids (Asn163, Arg294, and Arg298) and an amino acid with a hydroxyl group (Tyr447) of sPOMGNT2 make hydrogen bonds with the  $\beta$ - and  $\alpha$ -phosphates of UDP, respectively (Figure 1c and Appendix S1: Table S2). The uridine moiety of UDP is recognized by Glu324 by a hydrogen bond. The amino acid residues, Leu164, Thr295,

Gln296, Asn297, Ala347, and Gln348, surround UDP and contribute to the binding (Appendix S1: Table S3). Since UDP-GlcNAc is a donor substrate for POMGNT2, we considered that recognition of its  $\beta$ -phosphate would be important for the enzymatic activity. To confirm this, we constructed three alanine replacement mutants (N163A, R294A, and R298A), and measured their enzymatic activities. They completely lost the activity (Figure 1d), suggesting that these three charged amino acids are essential for the enzymatic reaction. In addition, for the enzymatic assay, divalent metal cations were not required for POMGNT2 activity (Appendix S1: Figure S3). It is consistent with the facts that glycosyltransferases belong to the GT-B family do not require a divalent cation for their activity (Nagae et al., 2020), and no metal ions were found in our crystal structures.

## 2.3 | Mannosyl peptide complex

Next, we investigated the recognition mechanism of specific *O*-Man by POMGNT2. Of the three specific *O*-Man positions, Thr317, Thr319, and Thr379, on  $\alpha$ -DG that can be modified by POMGNT2 (Hara et al., 2011; Yoshida-Moriguchi et al., 2010; Yagi et al., 2013), we focused on Thr379 because Thr317 and Thr319 are close to each other and thus mutating these residues may yield results that are difficult to interpret. Halmo *et al.* proposed that the RXR motif at the N-terminal side of the *O*-Man-modified residue contributes to the acceptor selectivity of POMGNT2 (Halmo et al., 2017). Therefore, to examine the importance of amino acid sequences at the N-terminal side of the *O*-Man-modified residue, we designed two *O*-mannosyl peptides with amino acid sequences around Thr379 (379Man long and 379Man short peptides, Table 1).

First, to compare the efficiency of these two *O*-mannosyl peptides as acceptors for POMGNT2, kinetic experiments were performed using increasing concentrations of each peptide and 20 mM UDP-GlcNAc. POMGNT2 activities in the presence of the 379Man long or short peptide followed typical Michaelis-Menten kinetics (Appendix S1: Figure S4), and the kinetic parameters were calculated by nonlinear regression analysis (Table 1). The  $K_m$  values,  $1.8 \pm 0.2$  mM for the 379Man long peptide and  $6.7 \pm 0.8$  mM for the 379Man short peptide, indicated that the affinity of POMGNT2 for the 379Man long peptide was higher than that for the 379Man short peptide. On the other hand, the  $k_{cat}$  value for the 379Man short peptide was higher than that for the 379Man long peptide, and the catalytic efficiencies ( $k_{cat}/K_m$ ) for the two *O*-mannosyl peptides were comparable. These results suggest that the amino acid sequences including the RXR motif at the N-terminal side of the *O*-Man-modified residue play a modest role in the affinity for POMGNT2, but are not essential for the enzyme activity.

To reveal the additional acceptor recognition mechanism of POMGNT2, the crystal structures of the sPOMGNT2, UDP,

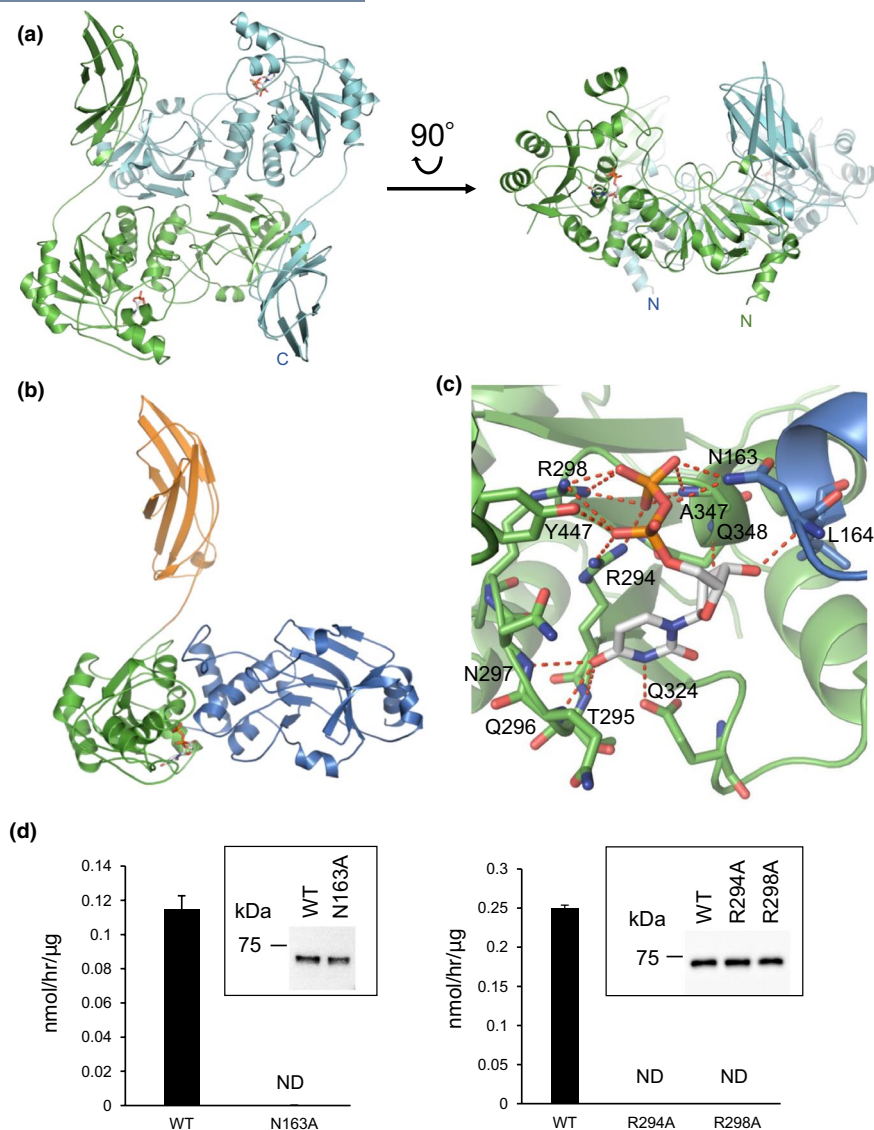


**FIGURE 1** Crystal structure of sPOMGNT2 and its interaction with UDP. (a) Overall structure of the sPOMGNT2 dimer. Each monomer is colored green and pale blue, and bound UDP molecules are shown in stick models. (b) Domain structure of the monomer. The N-terminal catalytic domain consists of an N-lobe (residues 53–277, blue) and C-lobe (residues 286–476, green). The C-terminal FnIII domain (residues 477–580) is colored orange. (c) Interaction between sPOMGNT2 and UDP. Side chains of the residues which interact with UDP are shown by stick models colored blue (N-lobe) and green (C-lobe). UDP is shown by a gray and orange stick model. Red dotted lines are hydrogen bonds. (d, left) Enzymatic activities of the WT and N163A mutant of sPOMGNT2. sPOMGNT2 immunoprecipitated from the cell lysate was used because the N163A mutant was scarcely secreted to the culture media. (d, right) Enzymatic activities of the WT, R294A, and R298A mutants of sPOMGNT2. sPOMGNT2 immunoprecipitated from the culture media was used. Insets: immunoblot analyses of sPOMGNT2 proteins to normalize input sPOMGNT2. ND means that the activities were not detected. Average values  $\pm$  SE of three independent experiments are shown

and *O*-mannosyl peptide (379Man short or long peptide) complexes were determined. The 379Man short complex contains two sPOMGNT2 molecules, two UDPs, and a peptide in an asymmetric unit, and the 379Man long complex contains four sPOMGNT2 molecules, four UDPs, and two peptides (Appendix S1: Table S4). The r.m.s.d. value between the nonpeptide and 379Man short complex structures was 0.393 Å, indicating little conformational change by the peptide binding (Appendix S1: Table S5). On the other hand, the values for the

379Man long complex were about 1.0 Å. This might have been caused by a crystallographic factor, because the space groups of the nonpeptide form and the 379Man short complex were both  $P2_12_12_1$ , but that of the 379Man long complex was  $P2_1$  (Appendix S1: Table S1). In the 379Man long complex, each peptide takes a different conformation; the orientation of one conformer is the same as that of the 379Man short structure (conformer 1), and the other conformer has an orientation opposite that of the 379Man short structure (conformer 2). The

**TABLE 1** Kinetic parameters of sPOMGNT2 with 379Man long or short peptide

	Amino acid sequence	$K_m$ (mM)	$V_{max}$ (nmol/hr/ $\mu$ g)	$k_{cat}$ (min <sup>-1</sup> )	$k_{cat}/K_m$ (mM <sup>-1</sup> min <sup>-1</sup> )
379Man long	Ac-TIRTRGAIQ(Man) TPTLGPIQPTR-NH <sub>2</sub>	1.8 ± 0.2	279 ± 7.7	298 ± 8.2	166
379Man short	Ac-Q(Man)TPTLGPIQPTR-NH <sub>2</sub>	6.7 ± 0.8	636 ± 39	680 ± 42	102

binding mode of conformer 2 is thought to be unimportant, because there is little interaction between sPOMGNT2 and conformer 2. Even the alanine-replaced mutant of Gln113, which is the only residue making a hydrogen bond in conformer 2, did not affect the enzymatic activity (Appendix S1: Figure S5). Therefore, we will describe the structures of 379Man short and 379Man long conformer 1.

## 2.4 | Recognition mechanism of mannosyl peptide

The nine N-terminal amino acid residues of the 379Man long peptide were disordered and could not be modeled in our crystal structure. The other region of the peptide interacts with sPOMGNT2 in the same way in the 379Man short and 379Man long complexes. One end of the peptide locates near the UDP-binding site, and the opposite end extends toward the FnIII domain of another protomer (Figure 2a). Because the resolution of the short peptide was better than that of the long peptide as judged from the electron density maps (Appendix S1: Figure S6), a subsequent detailed analysis of the recognition of the mannosyl peptide was performed using the 379Man short peptide.

Mannose and the surrounding amino acids of its peptide have many interactions with the catalytic domain of sPOMGNT2 (Figure 2b and Appendix S1: Table S6). Mannose interacts with His166 by a hydrogen bond and hydrophobic interaction, and with Cys436 by a hydrophobic interaction. Thr(2) at the base of mannose, Pro(3), and Thr(4) (the TPT motif) of the peptide interact with His125, Thr127, Phe159, Asn160, Phe247, and Cys437 by a hydrogen bond or hydrophobic interaction. To confirm the importance of these interactions for mannosylated substrate recognition, several alanine-substituted mutants at the respective amino acids were constructed and their enzymatic activities were measured. As shown in Figure 2d, the H166A and C436A mutants completely lost the activities, suggesting that direct recognition of mannose by the residues is essential for the acceptor substrate recognition. It was also shown that recognition of Thr(2), Pro(3), and Thr(4) by the catalytic domain is essential for POMGNT2, because the H125A, F159A, and C437A mutants completely lost their activities. These results indicate that the interactions at the TPT motif are critical for the acceptor substrate recognition.

Many interactions are also observed between mannosyl peptide and the FnIII domain of sPOMGNT2. Since mannose

is far from the FnIII domain, all of the interactions observed involved the peptide moiety. The residues of Trp525, Gln527, Asn532, Thr533, Tyr534, Leu557, Trp559, Phe572, and Val575 of sPOMGNT2 interact with the C-terminal region of the peptide from Pro(7) to Arg(12) mainly by hydrophobic interactions (Figure 2c, Appendix S1: Figure S7, and Appendix S1: Table S7). Asn532 forms additional hydrogen bonds between the peptide. To determine whether the interaction at the FnIII domain is required for acceptor substrate recognition, a mutant sPOMGNT2 lacking the C-terminal FnIII domain (T477Δ) was constructed. The mutant protein completely lost the enzymatic activity (Figure 2d), suggesting the importance of the FnIII domain for acceptor substrate recognition. It has been reported that a patient who harbored the R445Δ mutant in POMGNT2, which lacks the whole FnIII domain, showed serious symptoms of muscular dystrophy (Manzini et al., 2012). We prepared a R445Δ mutant protein and confirmed that its enzymatic activity was lost *in vitro* (Appendix S1: Figure S8). This demonstrated that the FnIII domain is essential for the function of POMGNT2.

Next, we focused on several characteristic interactions (Figure 2c)—namely, those involving Trp525, which makes a hydrophobic interaction with the side chain of Gln(9); Asn532, which forms hydrophobic and hydrogen bond interactions with Pro(10), Thr(11), and Arg(12); Tyr534, which forms a hydrophobic interaction with Pro(10); Trp559, which forms hydrophobic and CH- $\pi$  interactions with Pro(7), Ile(8), and Gln(9); and Phe572, which makes a hydrophobic interaction with the side chain of Gln(9). Mutant proteins in which each respective amino acid residue was changed to alanine were constructed, and their activities were measured (Figure 2d). W559A almost entirely lost its activity and W525A and F572A showed reduced activity. This suggests the importance of Trp559, which exhibits multiple interactions with peptide moieties. The mild reductions in activity displayed by the W525A and F572A mutants are consistent with the limited hydrophobic interactions observed in the structure. Likewise, the enzymatic activity of W534A was similar to that of the wild type, which is consistent with the extremely limited hydrophobic interactions with the peptide. The aromatic ring of Trp534 has a different angle from the pyrrolidine ring of Pro(10) and did not contribute to the peptide binding. Finally, the enzymatic activity of N532A was shown to be the same as that of the wild type, suggesting that the interaction with Pro(10), Thr(11), and Arg(12), which are located far from mannose, may not be important even though

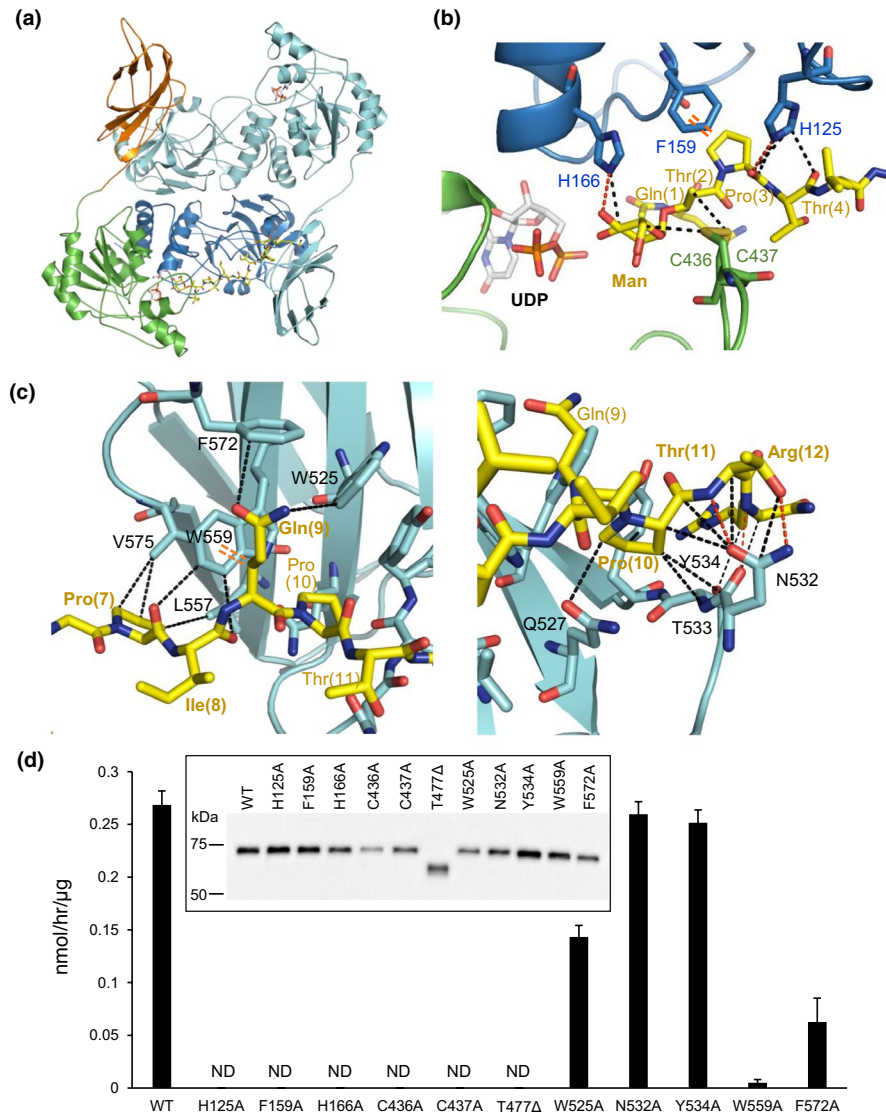


**FIGURE 2** Crystal structure of sPOMGNT2 with mannosyl peptide. (a) Overall structure of the sPOMGNT2-mannosyl peptide complex. Two UDP (gray and orange) and a 379Man short peptide (yellow) which are shown by stick models are in the sPOMGNT2 dimer. The different domains of one sPOMGNT2 molecule are colored as described in Figure 1b, and the other sPOMGNT2 molecule is colored pale blue. (b) Interaction between sPOMGNT2 and the 379Man short peptide in the region around mannose. The N-lobe and C-lobe of sPOMGNT2, mannosyl peptide, and UDP are shown by blue, green, yellow, and gray/orange color, respectively. The red and black dotted lines and an orange double dotted line are hydrogen bonds, hydrophobic interactions, and a CH- $\pi$  interaction, respectively. (c) Interaction between sPOMGNT2 and the C-terminal region of the 379Man short peptide. The FnIII domain of another molecule of sPOMGNT2 (pale blue) different from that shown in panel B interacts with the C-terminal region of the peptide (yellow). The types of interactions are shown in the same way as in panel (b). (d) Enzymatic activities of sPOMGNT2 mutants at which residues interact with mannosyl peptide. T477 $\Delta$  is a deletion mutant which lacks the whole C-terminal FnIII domain. sPOMGNT2 immunoprecipitated from the culture media was used. Inset: immunoblot analysis of sPOMGNT2 proteins to normalize input sPOMGNT2. ND means that the activities were not detected. Average values  $\pm$  SE of three independent experiments are shown

multiple numbers of hydrogen bonds and hydrophobic interactions are observed in the structure.

### 3 | DISCUSSION

In addition to a catalytic domain, POMGNT2 has an FnIII domain, which is found in mainly extracellular proteins; it plays

important functional roles through the formation of protein-protein interfaces (Campbell & Spitzfaden, 1994). We demonstrated that the mutant sPOMGNT2 lacking an FnIII domain lost the enzymatic activity, which clearly demonstrated that this domain is essential for its function (Figure 2d). Our structural study revealed that the FnIII domain protrudes to form a domain-swapped dimer (Figure 1a,b). The dimeric structure of sPOMGNT2 is functionally important because an acceptor

substrate is recognized by both the catalytic domain of one protomer and the FnIII domain of another protomer. This is why the deletion of the FnIII domain led to a loss of activity. Notably, this type of acceptor recognition is identical to our recent report on FKRP, which functions in the biosynthesis of the functional core M3-type glycan (Kuwabara et al., 2020). The acceptor substrate is recognized with different domains of two protomers of the dimer FKRP, which recognize one acceptor substrate. This style of sandwich recognition machinery may contribute to the specific recognition of the acceptor.

In studying the 379Man long peptide complex structure, we observed that the region of the N-terminal side of the *O*-mannosylation site was disordered and the structure could not be modeled. This suggests that the interaction between POMGNT2 and the N-terminal side of the acceptor mannosyl peptide is weak. Such a conclusion was also supported by the comparative kinetic study between 379Man long and short peptides (Table 1). While the  $K_m$  value of the long peptide for sPOMGNT2 was lower than that of the short peptide, the catalytic efficiencies for the two peptides were comparable. These observations suggest that the N-terminal side region plays a modest role in the affinity for POMGNT2 but is not essential for the enzyme activity. This is consistent with the finding of a previous study that the RXR motif at the N-terminal region of the acceptor peptide contributes to the acceptor selectivity of POMGNT2 (Halmo et al., 2017).

Mannose and its surrounding residues, Thr(2), Pro(3), and Thr(4) (the TPT motif) of the mannosyl peptide, are recognized by eight amino acid residues of the catalytic domain of POMGNT2: His125, Thr127, Phe159, Asn160, His166, Phe247, Cys436, and Cys437 (Figure 2b and Appendix S1: Table S6). Each of the sPOMGNT2 mutants that lacked an interaction with mannose or the TPT motif showed no enzymatic activity (Figure 2d). This indicates the importance of the precise spatial arrangement of the residues of POMGNT2 surrounding the mannose and the TPT motif of the acceptor substrate (catalytic domain interaction site as shown in Figure 3). It was reported that a patient who harbored an R158H mutation in POMGNT2 showed serious symptoms of muscular dystrophy (Manzini et al., 2012). We prepared the R158H mutant protein and confirmed that its enzymatic activity was lost *in vitro* (Appendix S1: Figure S8). Our analysis showed that the mutation disrupts the structure which is required for acceptor substrate recognition.

The mannosyl peptide is also recognized by the FnIII domain of sPOMGNT2 at its C-terminal region of the *O*-mannosylation site by hydrophobic and CH- $\pi$  interactions (Figure 2c, Appendix S1: Figure S7, and Appendix S1: Table S7). Mutational analysis of the FnIII domain of sPOMGNT2 showed a variety of effects on the enzymatic activity (Figure 2d). We demonstrated that mutant proteins of Trp525, Trp559, and Phe572, which interact with Pro(7),

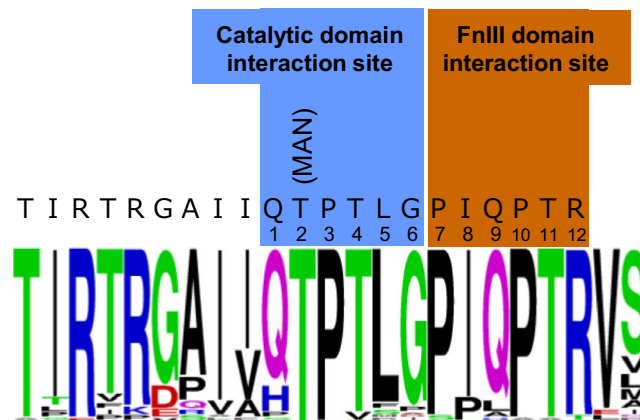


**FIGURE 3** Schematic model of POMGNT2 and mannosyl peptide. Conservation of amino acid sequences of the mannosylated sites of  $\alpha$ -DG at around residue 379 is presented at the bottom of the figure. The sequence alignment of 23-mer sequences of  $\alpha$ -DG from the same vertebrate orthologues of previous report (Halmo, 2017) was carried out by ConSurf program (Berezin, 2004). The amino acid sequence of the 379Man long peptide, which was used in this study, is on it. The number corresponding to the 379Man short peptide is shown between them. Areas shown in blue and brown boxes are regions interacting by the catalytic domain and FnIII domain of POMGNT2, respectively. Note that the two domains are from different molecules in the dimer

Ile(8), and Gln(9) of the mannosyl peptide, showed a reduction of enzymatic activities. The mutant proteins of Asn532 and Tyr534, which interact with Pro(10), Thr(11), and Arg(12) of the peptide, showed almost the same activity as the wild type. This suggests that, in the C-terminal region of the *O*-mannosyl peptide, residues in close proximity to mannose contribute to the binding. In addition, multiple hydrophobic and CH- $\pi$  interactions in this region contribute to the binding of the acceptor substrate (the FnIII domain interaction site, as shown in Figure 3), which is consistent with the general function of the FnIII domain, namely, the formation of protein-protein interfaces.

POMGNT2 forms a GlcNAc $\beta$ 1-4Man structure on *O*-mannosylated  $\alpha$ -DG at three specific positions: Thr317, Thr319, and Thr379. By considering both the amino acid sequences around mannose and the results of our structural analyses, we can gain insight into the mechanism by which POMGNT2 attaches GlcNAc to the specific sites on  $\alpha$ -DG. In the case of 317-TPT-319, both Thr317 and Thr319 are modified by addition of the core M3, in contrast to the case of 379-TPT-381, in which only Thr379 but not Thr381 is modified (Yoshida-Moriguchi et al., 2010). Since the following amino acid sequence of the former site is 317-TPTP-320 but that of the latter is 379-TPTL-382, Pro followed by (Man)Thr might be necessary for the modification by POMGNT2 (the catalytic domain interaction site, as shown in Figure 3). The FnIII domain of sPOMGNT2 is also required for the interaction at the C-terminal region of the mannosyl peptide (Figure 3).

However, a conserved motif among the C-terminal regions of the three *O*-mannosylation sites is not found (Appendix S1: Figure S9). It suggests that recognition of this region is achieved by a hydrophobic interaction on a specific three-dimensional structure. One possibility is that proline is the only amino acid that fixes the structure around the main chain, as such proline might contribute to the specific three-dimensional structure of this region.

A DALI search (Holm, 2020) revealed that there is no structure with overall similarity to POMGNT2, but the spatial arrangement of the catalytic residues of POMGNT2 was similar to that of *O*-linked  $\beta$ -*N*-acetylglucosamine transferase (OGT) (Appendix S1: Figure S10a). OGT transfers GlcNAc from the donor substrate, UDP-GlcNAc, to the Ser/Thr of acceptor proteins (Lazarus et al., 2011). The catalytic mechanism by which POMGNT2 transfers GlcNAc may be proposed based on our structural and mutational analyses and OGT study, because both enzymes belong to the GT-B glycosyltransferase family (Lazarus et al., 2011). Since His166, Arg294, and Arg298 surround  $\beta$ -phosphate of UDP in the sPOMGNT2 structure, they may play a role in the enzymatic reaction (Appendix S1: Figure S10a,b). At the beginning of the reaction, His166 receives hydrogen from the 4-hydroxyl group of mannose (step 1), the distance of 2.8 Å between them is sufficient. Then, the negatively charged oxygen of mannose attacks the 1 position of UDP-GlcNAc from the hydrogen side, and a GlcNAc $\beta$ 1-4Man bond is formed (step 2). After that, GlcNAc is released from UDP and then an additional negative charge remains at the  $\beta$ -phosphate of UDP (step 3). Arg294 and/or Arg298 donate protons to UDP to stabilize it, and the series of reactions ends (step 4). Notably, each Arg is important for the POMGNT2 activity (Figure 1d). However, it is difficult to judge which Arg residue is suitable as a proton donor, because the distances between the oxygen of  $\beta$ -phosphate and the nitrogens of Arg294 (2.8 Å) and Arg298 (2.7 Å and 2.9 Å) are very close. In the case of OGT, His498 receives a hydrogen from a Ser residue that is 3.5 Å away. The negatively charged oxygen of Ser attacks the 1 position of UDP-GlcNAc from the hydrogen side, and GlcNAc is released from UDP. Then, the negative charge remaining at the  $\beta$ -phosphate of UDP is neutralized by Lys842, which is 2.7 Å away from the oxygen of  $\beta$ -phosphate. The basic enzymatic reaction mechanism may be the same between POMGNT2 and OGT.

POMGNT2 transfers GlcNAc to mannosylated  $\alpha$ -DG to form the GlcNAc $\beta$ 1-4Man structure, which is a part of core M3. So far, the only protein known to be modified with core M3 is  $\alpha$ -DG. Here, we identified each amino acid of POMGNT2 which interacts with the corresponding mannose and its surrounding amino acid residues on the mannosyl peptide. The TPT motif and mannose are the most important for the recognition. In addition, both the N-terminal region including the RXR motif and the C-terminal hydrophobic interactions may determine the specific *O*-Man positions

on  $\alpha$ -DG recognized by POMGNT2. The FnIII domain of POMGNT2 is especially important for the hydrophobic interaction. Our study has delineated a new manner of glycan-linkage formation.

## 4 | EXPERIMENTAL PROCEDURES

Additional descriptions of experimental procedures used in the study are provided in Appendix S1.

### 4.1 | Materials

Mannosyl peptides (Table 1) were synthesized in a solid-phase manner using 9-fluorenyloxymethoxycarbonyl (Fmoc) chemistry with N<sup>2</sup>-(9-fluorenylmethoxycarbonyl)-*O*-{2,3,4,6-tetra-*O*-(*tert*-butoxycarbonyl)- $\alpha$ -D-mannopyranosyl}-threonine following the previously reported method (Tanaka et al., 2019).

### 4.2 | Protein expression, purification, crystallization, and structure determination

The luminal region of bovine POMGNT2 (sPOMGNT2, residues from 45 to the C-terminus, UniProt ID; Q5NDF2) was expressed by using a piggyBac transposon-based mammalian cell expression system that was kindly provided by Dr. James M. Rini (Li et al., 2013). Purification, crystallization, and structure determination of sPOMGNT2 were carried out by the procedure described in Appendix S1.

### 4.3 | Generation of sPOMGNT2 mutants and the enzymatic assay

The expression vector for the secreted type of human sPOMGNT2 (Arg24 to the C-terminus) was prepared to measure the enzymatic activities. The expressed proteins in HEK293T cells were isolated by anti-c-Myc antibody-agarose, and the agarose bound proteins were subjected to the enzymatic assay as described in Appendix S1.

## ACKNOWLEDGMENTS

We thank the beamline staffs of the Photon Factory (KEK, Tsukuba, Japan) and EMBL Hamburg at the PETRA III storage ring (DESY, Hamburg, Germany) for X-ray diffraction and data collection; Ms. T. Aoki (KEK) for her technical support; and Dr. T. Toda (University of Tokyo, Tokyo, Japan) for generously providing us the human sPOMGNT2 expression vector.



## AUTHOR CONTRIBUTIONS

R.I., N.K., H.M., T.E., and R.K. designed research; R.I., N.K., H.M., T.T., and M.M. performed research; R.I., N.K., H.M., and M.T. analyzed data; R.I., N.K., H.M., M.T., T.E., and R.K. wrote the paper.

## ORCID

Ryuichi Kato  <https://orcid.org/0000-0003-2087-2896>

## REFERENCES

- Berezin, C., Glaser, F., Rosenberg, J., Paz, I., Pupko, T., Fariselli, P., Casadio, R., & Tal-B. N. (2004). ConSeq: The identification of functionally and structurally important residues in protein sequences. *Bioinformatics*, *20*, 1322–1324.
- Breton, C., Šnajdrová, L., Jeanneau, C., Koča, J., & Imberty, A. (2006). Structures and mechanisms of glycosyltransferases. *Glycobiology*, *16*, 29R–37R. <https://doi.org/10.1093/glycob/cwj016>
- Campbell, I. D., & Spitzfaden, C. (1994). Building proteins with fibronectin type III modules. *Structure*, *2*, 333–337. [https://doi.org/10.1016/S0969-2126\(00\)00034-4](https://doi.org/10.1016/S0969-2126(00)00034-4)
- Chiba, A., Matsumura, K., Yamada, H., Inazu, T., Shimizu, T., Kusunoki, S., Kanazawa, I., Kobata, A., & Endo, T. (1997). Structures of sialylated *O*-linked oligosaccharides of bovine peripheral nerve  $\alpha$ -dystroglycan: The role of a novel *O*-mannosyl-type oligosaccharide in the binding of  $\alpha$ -dystroglycan with laminin. *Journal of Biological Chemistry*, *272*, 2156–2162. <https://doi.org/10.1074/jbc.272.4.2156>
- Endo, T. (2019). Mammalian *O*-mannosyl glycans: Biochemistry and glycopathology. *Proceedings of the Japan Academy. Series B, Physical and biological sciences*, *95*, 39–51.
- Halmó, S. M. Singh, D., Patel, S., Wang, S., Edlin, M., Boons, G. J., Moremen, K. W., & Wells, L. (2017). Protein *O*-linked mannosyl- $\beta$ -1,4-*N*-acetylglucosaminyl-transferase 2 (POMGNT2) is a gate-keeper enzyme for functional glycosylation of  $\alpha$ -dystroglycan. *Journal of Biological Chemistry*, *292*, 2101–2109.
- Hara, Y., Kanagawa, M., Kunz, S., Yoshida-Moriguchi, T., Satz, J. S., Kobayashi, Y. M., Zhu, Z., Burden, S. J., Oldstone, M. B. A., & Campbell, K. P. (2011). Like-acetylglucosaminyltransferase (LARGE)-dependent modification of dystroglycan at Thr-317/319 is required for laminin binding and arenavirus infection. *Proceedings of the National Academy of Sciences of the United States of America*, *108*, 17426–17431. <https://doi.org/10.1073/pnas.1114836108>
- Harrison, R., Hitchen, P. G., Panico, M., Morris, H. R., Mekhaiel, D., Pleass, R. J., Dell, A., Hewitt, J. E., & Haslam, S. M. (2012). Glycoproteomic characterization of recombinant mouse  $\alpha$ -dystroglycan. *Glycobiology*, *22*, 662–675. <https://doi.org/10.1093/glycob/cws002>
- Holm, L. (2020). DALI and the persistence of protein shape. *Protein Science*, *29*, 128–140. <https://doi.org/10.1002/pro.3749>
- Inamori, K. I., Endo, T., Gu, J., Matsuo, I., Ito, Y., Fujii, S., Iwasaki, H., Narimatsu, H., Miyoshi, E., Honke, K., & Taniguchi, N. (2004). *N*-Acetylglucosaminyltransferase IX acts on the GlcNAc $\beta$ 1,2-Man $\alpha$ 1-Ser/Thr moiety, forming a 2,6-branched structure in brain *O*-mannosyl glycan. *Journal of Biological Chemistry*, *279*, 2337–2340. <https://doi.org/10.1074/jbc.C300480200>
- Inamori, K. I., Yoshida-Moriguchi, T., Hara, Y., Anderson, M. E., Yu, L., & Campbell, K. P. (2012). Dystroglycan function requires xylosyl- and glucuronyltransferase activities of LARGE. *Science*, *335*, 93–96. <https://doi.org/10.1126/science.1214115>
- Kanagawa, M., Kobayashi, K., Tajiri, M., Many, H., Kuga, A., Yamaguchi, Y., Akasaka-Many, K., Furukawa, J.-I., Mizuno, M., Kawakami, H., Shinohara, Y., Wada, Y., Endo, T., & Toda, T. (2016). Identification of a post-translational modification with ribitol-phosphate and its defect in muscular dystrophy. *Cell Reports*, *14*, 2209–2223. <https://doi.org/10.1016/j.celrep.2016.02.017>
- Krissinel, E., & Henrick, K. (2007). Inference of macromolecular assemblies from crystalline state. *Journal of Molecular Biology*, *372*, 774–797. <https://doi.org/10.1016/j.jmb.2007.05.022>
- Kuwabara, N., Imae, R., Many, H., Tanaka, T., Mizuno, M., Tsumoto, H., Kanagawa, M., Kobayashi, K., Toda, T., Senda, T., Endo, T., & Kato, R. (2020). Crystal structures of fukutin-related protein (FKRP), a ribitol-phosphate transferase related to muscular dystrophy. *Nature Communications*, *11*, 303.
- Lairson, L. L., Henrissat, B., Davies, G. J., & Withers, S. G. (2008). Glycosyltransferases: Structures, functions, and mechanisms. *Annual Review of Biochemistry*, *77*, 521–555.
- Lazarus, M. B., Nam, Y., Jiang, J., Sliz, P., & Walker, S. (2011). Structure of human *O*-GlcNAc transferase and its complex with a peptide substrate. *Nature*, *469*, 564–567. <https://doi.org/10.1038/nature09638>
- Li, Z., Michael, I. P., Zhou, D., Nagy, A., & Rini, J. M. (2013). Simple piggyBac transposon-based mammalian cell expression system for inducible protein production. *Proceeding of the National Academy of Sciences of the United States of America*, *110*, 5004–5009.
- Many, H., Chiba, A., Yoshida, A., Wang, X., Chiba, Y., Jigami, Y., Margolis, R. U., & Endo, T. (2004). Demonstration of mammalian protein *O*-mannosyltransferase activity: Coexpression of POMT1 and POMT2 required for enzymatic activity. *Proceedings of the National Academy of Sciences of the United States of America*, *101*, 500–505. <https://doi.org/10.1073/pnas.0307228101>
- Many, H., & Endo, T. (2017). Glycosylation with ribitol-phosphate in mammals: New insights into the *O*-mannosyl glycan. *Biochimica Et Biophysica Acta*, *1861*, 2462–2472.
- Many, H., Yamaguchi, Y., Kanagawa, M., Kobayashi, K., Tajiri, M., Akasaka-Many, K., Kawakami, H., Mizuno, M., Wada, Y., Toda, T., & Endo, T. (2016). The muscular dystrophy gene *TMEM5* encodes a ribitol  $\beta$ 1,4-xylosyltransferase required for the functional glycosylation of dystroglycan. *Journal of Biological Chemistry*, *291*, 24618–24627. <https://doi.org/10.1074/jbc.M116.751917>
- Manzini, M. C., Tambunan, D. E., Hill, R. S., Yu, T. W., Maynard, T. M., Heinzen, E. L., Shianna, K. V., Stevens, C. R., Partlow, J. N., Barry, B. J., Rodriguez, J., Gupta, V. A., Al-Qudah, A. K., Eyaid, W. M., Friedman, J. M., Salih, M. A., Clark, R., Moroni, I., Mora, M., ... Walsh, C. A. (2012). Exome sequencing and functional validation in zebrafish identify *GTDC2* mutations as a cause of Walker-Warburg syndrome. *American Journal of Human Genetics*, *91*, 541–547.
- Maurer, L. M., Ma, W., & Mosher, D. F. (2015). Dynamic structure of plasma fibronectin. *Critical Reviews in Biochemistry and Molecular Biology*, *51*, 213–227.
- Morise, J., Kizuka, Y., Yabuno, K., Tonoyama, Y., Hashii, N., Kawasaki, N., Many, H., Miyagoe-Suzuki, Y., Takeda, S., Endo, T., Maeda, N., Takematsu, H., & Oka, S. (2014). Structural and biochemical characterization of *O*-mannose-linked human natural killer-1 glycan expressed on phosphacan in developing mouse brains. *Glycobiology*, *24*, 314–324. <https://doi.org/10.1093/glycob/cwt116>
- Nagae, M., Yamaguchi, Y., Taniguchi, N., & Kizuka, Y. (2020). 3D structure and function of glycosyltransferases involved in *N*-glycan maturation. *International journal of molecular sciences*, *21*, 437.

- Nilsson, J., Nilsson, J., Larson, G., & Grahn, A. (2010). Characterization of site-specific *O*-glycan structures within the mucin-like domain of  $\alpha$ -dystroglycan from human skeletal muscle. *Glycobiology*, *20*, 1160–1169. <https://doi.org/10.1093/glycob/cwq082>
- Praissman, J. L., Live, D. H., Wang, S., Ramiah, A., Chinoy, Z. S., Boons, G. J., Moremen, K. W., & Wells, L. (2014). B4GAT1 is the priming enzyme for the LARGE-dependent functional glycosylation of  $\alpha$ -dystroglycan. *eLife*, *3*, e03943. <https://doi.org/10.7554/eLife.03943>
- Sheikh, M. O., Halmo, S. M., & Wells, L. (2017). Recent advancements in understanding mammalian *O*-mannosylation. *Glycobiology*, *27*, 806–819. <https://doi.org/10.1093/glycob/cwx062>
- Stalnaker, S. H., Hashmi, S., Lim, J. M., Aoki, K., Porterfield, M., Sanchez, G. G., Wheeler, J., Ervasti, J. M., Bergmann, C., Tiemeyer, M., & Wells, L. (2010). Site mapping and characterization of *O*-glycan structures on  $\alpha$ -dystroglycan isolated from rabbit skeletal muscle. *Journal of Biological Chemistry*, *285*, 24882–24891.
- Tanaka, T., Shiraishi, M., Matsuda, A., & Mizuno, M. (2019). Efficient synthesis of *N*- and *O*-linked glycopeptides using acid-labile Boc groups for the protection of carbohydrate moieties. *Tetrahedron Letters*, *60*, 151106.
- Willer, T., Inamori, K. I., Venzke, D., Harvey, C., Morgensen, G., Hara, Y., Beltrán Valero de Bernabé, D., Yu, L., Wright, K. M., & Campbell, K. P. (2014). The glucuronyltransferase B4GAT1 is required for initiation of LARGE-mediated  $\alpha$ -dystroglycan functional glycosylation. *eLife*, *3*, e03941. <https://doi.org/10.7554/eLife.03941>
- Yagi, H., Nakagawa, N., Saito, T., Kiyonari, H., Abe, T., Toda, T., Wu, S. W., Khoo, K. H., Oka, S., & Kato, K. (2013). AGO61-dependent GlcNAc modification primes the formation of functional glycans on  $\alpha$ -dystroglycan. *Scientific Reports*, *3*, 3288.
- Yoshida, A., Kobayashi, K., Manya, H., Taniguchi, K., Kano, H., Mizuno, M., Inazu, T., Mitsuhashi, H., Takahashi, S., Takeuchi, M., & Herrmann, R. (2001). Muscular dystrophy and neuronal migration disorder caused by mutations in a glycosyltransferase, POMGnT1. *Developmental Cell*, *1*, 717–724.
- Yoshida-Moriguchi, T., Willer, T., Anderson, M. E., Venzke, D., Whyte, T., Muntoni, F., Lee, H., Nelson, S. F., Yu, L., & Campbell, K. P. (2013). SGK196 is a glycosylation-specific *O*-mannose kinase required for dystroglycan function. *Science*, *341*, 896–899.
- Yoshida-Moriguchi, T., & Campbell, K. P. (2015). Matriglycan: A novel polysaccharide that links dystroglycan to the basement membrane. *Glycobiology*, *25*, 702–713. <https://doi.org/10.1093/glycob/cwv021>
- Yoshida-Moriguchi, T., Yu, L., Stalnaker, S. H., Davis, S., Kunz, S., Madson, M., Oldstone, M. B. A., Schachter, H., Wells, L., & Campbell, K. P. (2010). *O*-mannosyl phosphorylation of alpha-dystroglycan is required for laminin binding. *Science*, *327*, 88–92. <https://doi.org/10.1126/science.1180512>

## SUPPORTING INFORMATION

Additional supporting information may be found online in the Supporting Information section.

**How to cite this article:** Imae R, Kuwabara N, Manya H, et al. The structure of POMGNT2 provides new insights into the mechanism to determine the functional *O*-mannosylation site on  $\alpha$ -dystroglycan. *Genes Cells*. 2021;26:485–494. <https://doi.org/10.1111/gtc.12853>